

Blood oxygenation level-dependent (BOLD) functional MRI of visual stimulation in the rat retina at 11.7 T

Bryan H. De La Garza^a, Eric R. Muir^{a,b}, Guang Li^{a,c}, Yen-Yu I. Shih^a and Timothy Q. Duong^{a-g,*}

Although optically based imaging techniques provide valuable functional and physiological information of the retina, they are mostly limited to the probing of the retinal surface and require an unobstructed light path. MRI, in contrast, could offer physiological and functional data without depth limitation. Blood oxygenation level-dependent functional MRI (BOLD fMRI) of the thin rat retina is, however, challenging because of the need for high spatial resolution, and the potential presence of eye movement and susceptibility artifacts. This study reports a novel application of high-resolution ($111 \times 111 \times 1000 \mu\text{m}^3$) BOLD fMRI of visual stimulation in the anesthetized rat retina at 11.7 T. A high-field MRI scanner was utilized to improve the signal-to-noise ratio, spatial resolution and BOLD sensitivity. Visual stimuli (8 Hz diffuse achromatic light) robustly increased BOLD responses in the retina [$5.0 \pm 0.8\%$ from activated pixels and $3.1 \pm 1.1\%$ from the whole-retina region of interest (mean \pm SD), $n = 12$ trials on six rats, $p < 0.05$ compared with baseline]. Some activated pixels were detected surrounding the pupil and ciliary muscle because of accommodation reflex to visual stimuli, and were reduced with atropine and phenylephrine eye drops. BOLD fMRI scans without visual stimulations showed no significantly activated pixels (whole-retina BOLD changes were $0.08 \pm 0.34\%$, $n = 6$ trials on five rats, not statistically different from baseline, $p > 0.05$). BOLD fMRI of visual stimulation has the potential to provide clinically relevant data to probe hemodynamic neurovascular coupling and dysfunction of the retina with depth resolution. Copyright © 2010 John Wiley & Sons, Ltd.

Keywords: laminar specificity; high magnetic field; high-resolution fMRI; choroid; dark and light adaptation; blood flow

INTRODUCTION

The retina, a sensory tissue located at the back of the eye, is the first stage of visual processing. It contains millions of photoreceptors that capture photons and convert them into electrical signals which travel along the optic nerve to the brain before they are turned into images. The entire retinal thickness, including the choroid vascular layer, is approximately $270 \mu\text{m}$ in rats (1). Many blinding diseases affect the retina.

Electroretinography (2) records electrical activities from various cell types in the retina via surface electrodes. Laser Doppler flowmetry (3), laser speckle imaging (4,5) and intrinsic optical imaging (6–8) can image hemodynamic (blood flow and oxygenation) changes associated with visual stimulations and physiological modulations. These imaging methods provide a means to investigate the unique neurovascular coupling in the retina (9,10), which is important because perturbations in neurovascular coupling and function have been implicated in many retinal diseases, including glaucoma (11–13) and diabetic retinopathy (10).

Hemodynamic responses to visual stimuli using other imaging techniques are sparse. Laser Doppler flowmetry reported visually evoked blood flow changes in the retina in the optic nerve head (14). Intrinsic optical imaging also reported visually evoked changes in the retina (6–8), although the signal source remains ambiguous, but is generally referred to as the 'reflectance change' caused by both scattering and absorption. Although these optical techniques provide valuable functional and

* Correspondence to: T. Q. Duong, Research Imaging Institute, UTHSCSA, 8403 Floyd Curl Dr., San Antonio, TX 78229, USA.
E-mail: duongt@uthscsa.edu

a B. H. D. E. La Garza, E. R. Muir, G. Li, Y.-Y. I. Shih, T. Q. Duong
Research Imaging Institute, University of Texas Health Science Center, San Antonio, TX, USA

b E. R. Muir, T. Q. Duong
Department of Biomedical Engineering, Georgia Institute of Technology, Atlanta, GA, USA

c G. Li, T. Q. Duong
Department of Radiology, University of Texas Health Science Center, San Antonio, TX, USA

d T. Q. Duong
Department of Ophthalmology, University of Texas Health Science Center, San Antonio, TX, USA

e T. Q. Duong
Department of Physiology, University of Texas Health Science Center, San Antonio, TX, USA

f T. Q. Duong
South Texas Veterans Health Care System, San Antonio, TX, USA

g T. Q. Duong
Southwest National Primate Research Center, San Antonio, TX, USA

Abbreviations used: BOLD, blood oxygenation level-dependent; EPI, echo planar imaging; fMRI, functional MRI; FOV, field of view; PVE, partial volume effect; SNR, signal-to-noise ratio.

physiological information of the retina, they are mostly limited to the probing of the retinal surface and require an unobstructed light path. The retinal pigment epithelium is generally inaccessible by optics. Diseases with media opacity, such as cataract and vitreous hemorrhage, may preclude the use of optics to study the retina.

MRI, in contrast, offers non-invasive physiological and functional data with depth resolution, albeit at a lower spatial resolution compared with optics. Oxygenation changes associated with physiological challenges in normal and degenerated retina have been reported using blood oxygenation level-dependent functional MRI (BOLD fMRI) at $90 \times 90 \times 1000 \mu\text{m}^3$ (1). Blood flow and its responses to physiological challenges in normal and degenerated retina (15,16) have been reported using MRI at $90 \times 90 \times 1500 \mu\text{m}^3$. These approaches offer a means to investigate neurovascular coupling associated with physiological challenges. MRI of light and dark adaptation has been reported using manganese-enhanced MRI, in which manganese serves as a calcium analog and an MRI contrast agent (17). BOLD fMRI of visual stimulation of the cat retina at $485 \times 485 \times 2000 \mu\text{m}^3$ found robust responses to visual stimuli and differential responses among stationary gratings, drifting gratings and dark (18).

In the present study, we explored the feasibility of performing BOLD fMRI of visual stimulation on the rat retina. Gradient-echo BOLD fMRI at 11.7 T was utilized. Visual stimuli employed diffuse achromatic light flickering at 8 Hz. A high magnetic field was used to improve spatial resolution and BOLD contrast sensitivity. The novelty of this study included BOLD fMRI of visual stimuli in rat retina for the first time at considerably higher resolution ($111 \times 111 \times 1000 \mu\text{m}^3$) and at high field (11.7 T). The challenges of visually evoked BOLD fMRI of the rat retina are discussed, and the solutions detailed. This approach could provide a means to study neurovascular coupling and function in the rat retina, where many retinal disease models are readily available.

MATERIALS AND METHODS

Animal preparation

All animal experiments were performed with institutional approval and in accordance with the Statement for the Use of Animals in Ophthalmic and Vision Research. Normal adult male Sprague Dawley rats (250–350 g) were initially anesthetized with approximately 2% isoflurane in air, intubated and mechanically ventilated. Afterwards, the animals were secured in an MRI-compatible rat stereotaxic headset with ear and tooth bars, and isoflurane was reduced to 0.9–1.0% after animals had been paralyzed with pancuronium bromide (3 mg/kg first dose, 1.5 mg/kg/h, intraperitoneal injection) (1,15). This animal preparation protocol yielded stable MRI data over a long acquisition time (1,15). End-tidal CO_2 was monitored via a Surgivet capnometer (Smith Medical, Waukesha, WI, USA). Noninvasive end-tidal CO_2 values have been calibrated previously against invasive blood gas samplings under an identical setting (19). The rectal temperature was maintained at $37.0 \pm 0.5^\circ\text{C}$. The heart rate and blood oxygen saturation level were monitored using a MouseOx system (STARR Life Science Corp., Oakmont, PA, USA). All recorded physiological parameters were maintained within normal physiological ranges. This animal protocol has been utilized previously, and has been demonstrated to yield robust BOLD responses to physiological challenges (1).

Animals were studied without ($n=5$) and with ($n=5$) the application of atropine, phenylephrine and proparacaine eye drops in different animals. In addition, fMRI studies were performed before and after eye drop application in two additional rats and the same setting, where the animal was slid out and back into the scanner without re-shim (remote administration without moving the animals was attempted, but the eye drop left a very bright spot on the images). Experiments were also performed without visual stimuli to evaluate potential 'correlation' noises from the animals mentioned above. Proparacaine, which is a topical anesthetic with a half-life of 15 min, was not expected to have a significant effect during MRI acquisition. All eyes were coated with a thin layer of eye ointment to prevent dryness during MRI.

Visual stimulation

Visual stimuli used 8 Hz flickering achromatic light delivered via an optical fiber and a custom-made diffuser. A luminance of $72.64 \text{ candela/m}^2$ was measured in front of the rat eye. For each trial, fMRI data were acquired with 10 epochs of (60 s OFF and 30 s ON), followed by 60 s OFF. In a few earlier experiments, five epochs of (60 s OFF and 30 s ON), followed by 180 s of OFF, were used. A 5–10-min break (no visual stimulation) was given between repeated trials. The timing of the stimuli, frequency and amplitude were controlled by a PC with custom-made software/hardware. Typically, two to four trials were repeated on each animal.

MRI methods

MRI studies were performed on an 11.7-T/16-cm magnet and a 75-G/cm B-GA9S gradient insert (Bruker, Billerica, MA, USA). A custom-made, small circular transceiver surface coil (inside diameter, $\sim 7 \text{ mm}$) was placed on the left eye. Magnetic field homogeneity was optimized using standard FASTMAP shimming with first-order shims on an isotropic voxel of $7.5 \times 7.5 \text{ mm}^2$ encompassing the entire eye ball. The magnet bore was dark except during visual stimulation.

Scout images were acquired to plan a single mid-sagittal imaging slice bisecting the center of the eye for all subsequent imaging in order to minimize the partial volume effect (PVE) caused by retinal curvature (1,15). BOLD fMRI was acquired using single-shot, gradient-echo, echo planar imaging (EPI) with inversion recovery contrast, employing $\text{TR}=3 \text{ s}$, $\text{TE}=13 \text{ ms}$, $\text{TI}=1.3 \text{ s}$, spectral width = 200 kHz, a single $1000\text{-}\mu\text{m}$ -thick slice, matrix = 90×90 and field of view (FOV) = $10 \times 10 \text{ mm}^2$ ($111 \times 111 \times 1000 \mu\text{m}^3$). The vitreous signal was suppressed using inversion recovery (18).

At $111 \times 111 \times 1000 \mu\text{m}^3$, two to three pixels spanned the retinal thickness of $267 \mu\text{m}$, including the choroid (1). Assuming a spherical rat eye of 6 mm in diameter, the upper limit of PVE caused by the retinal curvature was 16% of the total retinal thickness for a single central imaging slice (1).

Anatomical images were also acquired with and without eye drops using a gradient-echo sequence, $\text{TR}=360 \text{ ms}$, $\text{TE}=3 \text{ ms}$, matrix = 128×128 , FOV = $8.3 \times 8.3 \text{ mm}^2$, slice thickness = 0.6 mm and three consecutive slices ($65 \times 65 \times 600 \mu\text{m}^3$).

Data analysis

Data analysis used codes written in MATLAB[®] (MathWorks Inc., Natick, MA, USA) and STIMULATE (University of Minnesota)

software. Images were acquired in time series, and corrected for potential motion and image drift before additional analysis (1). Low-frequency drifting of the BOLD time series was corrected using a band-stop filter (0.001–0.01 Hz). BOLD fMRI analysis employed cross-correlation analysis to the ON/OFF block paradigm without convolving with a hemodynamic response function. Activation maps were calculated, color-coded and overlaid on echo planar images. For display purposes, the cross-correlation coefficient scale bars were set at 0.03–0.3 for all figures with 23 neighboring clustering. No mask was used. Time courses were obtained from activated pixels. Percentage changes were tabulated for active pixels on the retina as well as the region of interest (ROI) of the entire retina to avoid bias. Reported values were in means \pm standard deviation (SD). All statistical tests employed Student *t*-test, with $p < 0.05$ indicating statistical significance.

RESULTS

Figure 1 shows the anatomical images of an animal without eye drops and one with eye drops. The ciliary muscles were pulled back. The pupil was dilated and remained dilated at the end of the MRI experiments.

Figure 2 shows the visually evoked BOLD fMRI activation map and time course of a rat retina before and after application of atropine and phenylephrine eye drops in the same animals. Before eye drop application, activated pixels in the retinas and ciliary muscles were consistently detected (horizontal blue arrows). The animal was slid out of the scanner and eye drops were applied and the animal was slid back in without re-shimming. After eye drop application, activated pixels in the ciliary muscles were eliminated. Moreover, time-series movies of anatomical and functional MRI images showed that the pupils and ciliary muscles moved in correlation with the stimulus onset

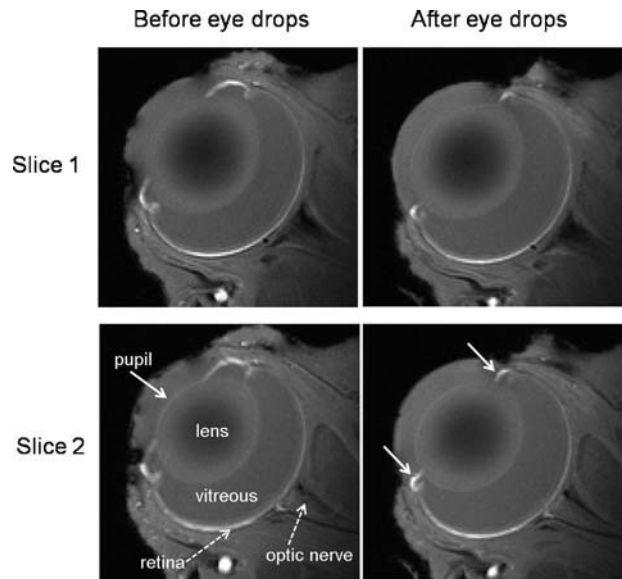


Figure 1. Anatomical images of the eye before and after eye drops (atropine and phenylephrine) in the same animal. Two consecutive image slices from a representative animal are shown. With eye drops, the pupil was dilated and the ciliary muscles, a ring of striated smooth muscle that controls accommodation, were pulled back.

before eye drops; these movements were markedly reduced or eliminated after the application of eye drops. It should be noted that activated pixels in the anterior chamber were sometimes detected, probably as a result of susceptibility artifacts (vertical green arrows).

As negative controls to confirm that activated pixels were free of 'correlation noise,' fMRI data were compared with and without visual stimulation on the same animals using identical acquisition and analysis protocols. Without visual stimulation, no significantly

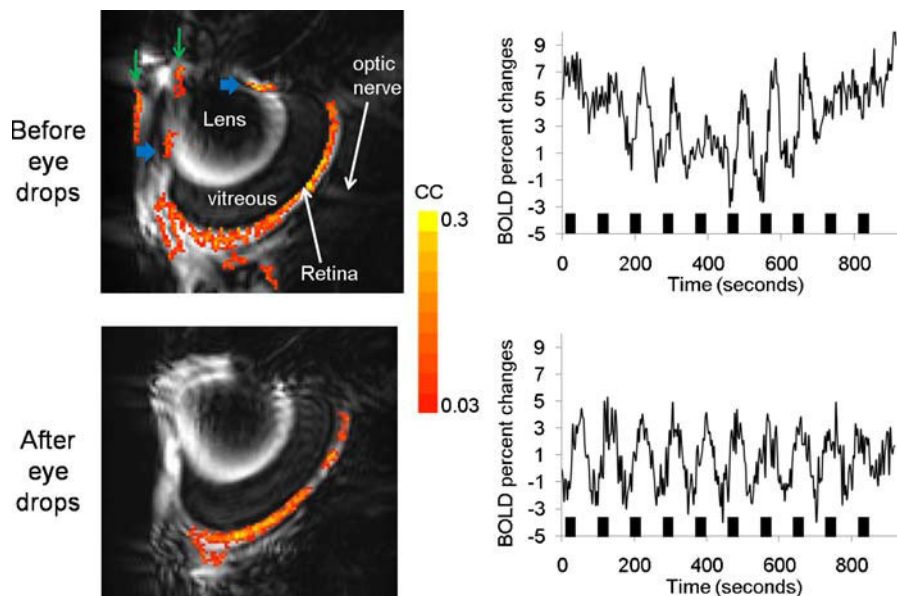


Figure 2. Visually evoked blood oxygenation level-dependent functional MRI (BOLD fMRI) activation map ($111 \times 111 \times 1000 \mu\text{m}^3$) of the same rat retina before and after application of atropine and phenylephrine eye drops in the same animal. Map is overlaid on echo planar images. Before eye drop application, activated pixels in the retinas and in the ciliary muscles (horizontal blue arrows) were detected. After eye drop application, activated pixels in the ciliary muscles were eliminated. Activated pixels in the anterior chamber (vertical green arrows) were probably artifacts. The stimulation paradigm involved 10 epochs of (60 s OFF and 30 s ON), followed by 180 s OFF. Color bar, cross-correlation coefficients of 0.03–0.3 (16 contiguous pixel clustering).

activated pixels were detected at the same statistical threshold (Fig. 3) and BOLD changes of the whole-retina ROI were $0.08 \pm 0.34\%$ (mean \pm SD, $n = 6$ trials on five rats), not statistically different from baseline ($p > 0.05$). Note that visual responses were sometimes stronger in the bottom half of the retina, because of the radiofrequency coil nonuniformity caused by coil positioning, which is most evident in the anatomical MR image of Fig. 1.

Figure 4 shows the BOLD fMRI activation map and the corresponding time course of a representative animal with application of atropine and phenylephrine eye drops and optimized shimming to minimize signal dropout and distortion of EPI. Activated pixels were predominantly localized to the retina without activated pixels in the pupils and ciliary muscles. The group-averaged percentage change from activated pixels in the retina was $5.0 \pm 0.8\%$ (mean \pm SD, $n = 12$ repeats on six rats, $p < 0.05$ compared with baseline). Data were also analyzed using an ROI of the entire retina. The group-average percentage change

from the whole-retina ROI was $3.1 \pm 1.1\%$ (mean \pm SD, $n = 12$ repeats on six rats, $p < 0.05$ compared with baseline).

DISCUSSION

This study demonstrates high-resolution BOLD fMRI of visual stimulation on the rat retina with $111 \times 111 \times 1000 \mu\text{m}^3$ at 11.7 T. Activated pixels in the ciliary muscles were reduced with atropine and phenylephrine eye drops. BOLD fMRI of the retina provides depth-resolved, clinically relevant information, and could be used to study normal retinal function as well as dysfunction in diseased states.

Animal issues

Eye motion

In contrast with optically based imaging techniques which have remarkably high temporal resolution, fMRI data per time point take on the order of seconds to acquire, depending on the spatial resolution, signal-to-noise ratio (SNR), pulse sequences and others. In addition, fMRI requires time-series acquisitions during which multiple epochs of baseline and stimulation are presented. Such fMRI studies take on the order of minutes, depending on stimulation paradigms. Moreover, multiple fMRI trial measurements and multiple modalities (such as functional, blood flow and anatomical MRI) can be made in the same setting. Thus, the elimination of eye movement in animal studies over hours is desirable for within comparisons. We have observed previously that, despite the animals being under deep isoflurane anesthesia *per se* (up to 3% isoflurane) (20), the eye still drifts slightly over time. This is probably because the eyeball could not be readily immobilized, in contrast with the skull for brain imaging. Paralytics as utilized herein successfully eliminated eye movement over long (hours) measurements. Residual drift can be readily corrected using image registration algorithms (20).

Without using eye drops, activations in the ciliary muscles and the lens were often observed to correlate with the activation paradigm. This is a result of physiologically induced changes from visual stimuli, known as 'accommodation reflex responses'. Atropine and phenylephrine were used to dilate the pupil and relax ciliary muscles, which could be seen in the anatomical MR image. Atropine is an antagonist for the muscarinic acetylcholine receptor (21), which blocks the activity of muscle and glands innervated by the parasympathetic nervous system and paralyzes the accommodation reflex, resulting in long-lasting pupil dilation (up to a few hours to a day). Phenylephrine is an agonist for α_1 -adrenergic receptors and activates the sympathetic nervous system, also resulting in pupil dilation (22). It is worth noting that it is possible that, with pupil dilation, more light will enter the retina, resulting in larger BOLD changes; such effects were not investigated.

Activated pixels in the anterior chamber were sometimes observed. Analysis of EPI movies showed that these activated pixels in the anterior chamber were fluctuating largely in intensity, but there were also minor changes in morphology localized to the anterior chamber (the retina, by and large, was not affected). This was probably a result of the temporal fluctuation of EPI in regions of high magnetic susceptibility and wrap-around (aliasing) caused by the small FOV used to achieve high resolution.

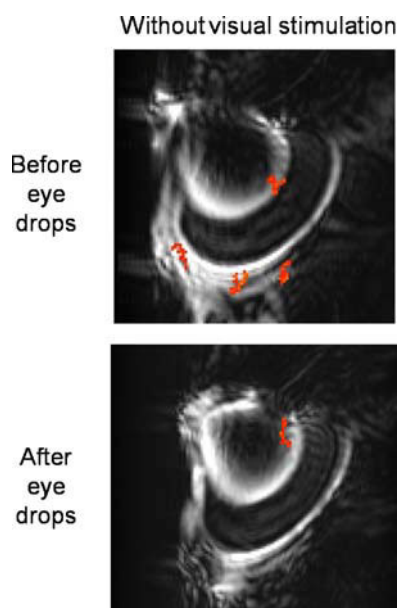


Figure 3. Identical experiments on the same animals as in Fig. 2, except with no visual stimulation.

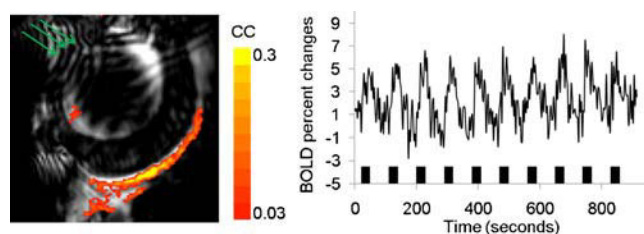


Figure 4. Blood oxygenation level-dependent functional MRI (BOLD fMRI) activation maps ($111 \times 111 \times 1000 \mu\text{m}^3$) of visual stimulation. After optimization, including voxel shimming and the application of eye drops, the retina appeared rounder (its normal shape). Activated pixels were clearly detected in the retina, but not in the ciliary muscles. The stimulation paradigm involved 10 epochs of (60 s OFF and 30 s ON). Color bar, cross-correlation coefficients of 0.03–0.3 (16 contiguous pixel clustering). The green arrows indicate the wrap-around as a result of using a small field of view, but this does not significantly affect the retina.

Anesthetics

Isoflurane was chosen over injectable anesthetics because it is readily adjustable and can be maintained at a stable level over an extended period, such that physiological parameters can be consistently maintained within the normal physiological ranges (23). Importantly, isoflurane anesthesia can be used in survival studies, in contrast with other commonly used anesthetics, such as α -chloralose and urethane. Paralytic can be effectively reversed by neostigmine, although it was not utilized here. The disadvantage of isoflurane is that it is a strong neural suppressor in a dose-dependent manner, which could reduce response magnitudes, similar to many other anesthetics. Isoflurane is also known to be a strong vasodilator, which could reduce the head room for stimulus-evoked blood flow, and thus the BOLD signal increase. Nonetheless, robust BOLD fMRI of visual stimulations in the retina could be detected under isoflurane. Robust BOLD fMRI in the brain has also been reported under isoflurane anesthesia (23–25). It is worth noting that medetomidine (Domitor[®]) (26,27) has recently gained some popularity in survival fMRI studies, because it also yields a robust BOLD response, although it is relatively difficult to maintain stable anesthesia over an extended period.

MRI issues

High-resolution MRI has low SNR; therefore, a high-sensitivity surface coil optimized for imaging the eye and a high magnetic field scanner were used to improve SNR. At high field, distortion and susceptibility-induced signal dropout are potential issues. Optimizations of shimming and EPI parameters are important. Echo planar images were relatively free of artifacts, although elongation or compression of the images (depending on the phase-encoding direction) and signal dropout in the anterior chambers in the retina (depending on shimming) were sometimes observed. Spin-echo EPI BOLD acquisition could minimize signal dropout (1) and, with spin echo acquisition, diffusion could be used to preferentially suppress vitreous signals (1). Non-EPI approaches that have less susceptibility and signal dropout artifacts, such as balanced steady-state free precession, could be explored.

In the brain, the stimulus-evoked BOLD change is typically around 1–3%. High-field MRI was used to improve BOLD contrast (28). BOLD percentage changes scale with field strengths. Physiological noises, however, become more apparent at higher fields. Nonetheless, there is a general consensus that BOLD contrast-to-noise ratio scales with B_0 (28).

Responses to visual stimulation

The group-averaged percentage change from activated pixels in the retina was $5.0 \pm 0.8\%$ and from the whole-retina ROI was $3.1 \pm 1.1\%$. ROI analysis was performed to avoid bias and to allow quantitative comparison with data without turning on the visual stimulation. Our findings are in general qualitative agreement with a previous study on BOLD fMRI of visual responses in the cat retina, also using inversion suppression of the vitreous humor at 9.4 T at $485 \times 485 \times 2000 \mu\text{m}^3$ (18). In that study, BOLD fMRI signals were reported to increase by $2.0 \pm 0.3\%$ as a result of drifting gratings and $1.0 \pm 0.1\%$ as a result of stationary gratings ($p < 0.02$). Higher field and higher spatial resolution generally yield larger BOLD responses as expected.

In a previous study using BOLD fMRI at $90 \times 90 \times 1000 \mu\text{m}^3$ (1), differential lamina-specific responses in the retina were detected, associated with physiological (hyperoxic and hypercapnic) challenges, which are known to induce vascular-specific responses. Similar findings have also been reported using blood flow fMRI (29) and blood volume fMRI (30) associated with the same physiological challenges. In the current study, the spatial resolution was lower than that of physiological stimulation (1) and the visual stimulus (flicker) did not evoke lamina-specific responses. Future studies will improve the spatial resolution and employ known lamina-specific visual stimuli to attempt to resolve lamina-specific responses in the retina.

CONCLUSIONS

This study demonstrates a novel BOLD fMRI application of visual stimulation on the rat retina at 11.7 T. Potential applications of BOLD fMRI include imaging of neurovascular coupling and function in normal and diseased states in animal models, such as diabetic retinopathy, glaucoma and macular degeneration. BOLD fMRI of the retina has the potential to complement existing retinal imaging techniques.

Acknowledgements

The authors thank Bill Rogers of the Research Imaging Institute for building the visual stimulation unit used in this study, Dr Joseph M. Harrison of Ophthalmology for his help with luminance measurements, and Dr Carlos Rosende of Ophthalmology for helpful discussions. This work was supported by the National Institutes of Health (R01EY014211, R01EY018855) and VA MERIT.

REFERENCES

1. Cheng H, Nair G, Walker TA, Kim MK, Pardue MT, Thule PM, Olson DE, Duong TQ. Structural and functional MRI reveals multiple retinal layers. *Proc. Natl. Acad. Sci. USA*. 2006; 103: 17,525–17,530.
2. Brown KT, Wiesel TN. Localization of the origins of the electroretinogram components by intraretinal recording in the intact cat eye. *J. Physiol.* 1961; 158: 257.
3. Riva CE, Grunwald JE, Sinclair SH. Laser Doppler velocimetry study of the effect of pure oxygen breathing on retinal blood flow. *Invest. Ophthalmol. Vis. Sci.* 1983; 24: 47–51.
4. Cheng H, Duong TQ. Simplified laser-speckle-imaging analysis method and its application to retinal blood flow imaging. *Opt. Lett.* 2007; 32: 2188–2190.
5. Cheng H, Yan Y, Duong TQ. Temporal statistical analysis of laser speckle image and its application to retinal blood-flow imaging. *Optics Express*, 2008; 16: 10,214–10,219.
6. Grinvald A, Bonhoeffer T, Vanzetta I, Pollack A, Aloni E, Ofri R, Nelson D. High-resolution functional optical imaging: from the neocortex to the eye. *Ophthalmol. Clin. North Am.* 2004; 17: 53–67.
7. Tsunoda K, Oguchi Y, Hanazono G, Tanifuji M. Mapping cone- and rod-induced retinal responsiveness in macaque retina by optical imaging. *Invest. Ophthalmol. Vis. Sci.* 2004; 45: 3820–3826.
8. Tso DY, Schallek J, Mzarella M, Ghim M, Abramoff M, Kwon Y, Kardon R, Pokorny J, Soliz P. *Pharmacological Dissection of Laminar Contributions to Intrinsic Optical Signals in the Retina*. Association for Research in Vision and Ophthalmology: Fort Lauderdale, FL, 2006; 5899.
9. Pournaras CJ, Rungger-Brandle E, Riva CE, Hardarson SH, Stefansson E. Regulation of retinal blood flow in health and disease. *Prog. Retin. Eye Res.* 2008; 27: 284–330.
10. Riva CE, Falsini B. Functional laser Doppler flowmetry of the optic nerve: physiological aspects and clinical applications. *Prog. Brain Res.* 2008; 173: 149–163.

11. Gugleta K, Fuchsjager-Mayrl G, Orgul S. Is neurovascular coupling of relevance in glaucoma? *Surv. Ophthalmol.* 2007; 52 (Suppl 2): S139–143.
12. Metea MR, Newman EA. Glial cells dilate and constrict blood vessels: a mechanism of neurovascular coupling. *J. Neurosci.* 2006; 26: 2862–2870.
13. Metea MR, Kofuji P, Newman EA. Neurovascular coupling is not mediated by potassium siphoning from glial cells. *J. Neurosci.* 2007; 27: 2468–2471.
14. Riva CE, Harino S, Shonat RD, Petrig BL. Flicker evoked increase in optic nerve head blood flow in anesthetized cats. *Neurosci. Lett.* 1991; 128: 291–296.
15. Li Y, Cheng H, Duong TQ. Blood-flow magnetic resonance imaging of the retina. *Neuroimage.* 2008; 39: 1744–1751.
16. Li Y, Cheng H, Shen Q, Kim M, Thule PM, Olson DE, Pardue MT, Duong TQ. Blood-flow magnetic resonance imaging of retinal degeneration. *Invest. Ophthalmol. Vis. Sci.* 2009; 50: 1824–1830.
17. Berkowitz BA, Roberts R, Goebel DJ, Luan H. Noninvasive and simultaneous imaging of layer-specific retinal functional adaptation by manganese-enhanced MRI. *Invest. Ophthalmol. Vis. Sci.* 2006; 47: 2668–2674.
18. Duong TQ, Ngan S-C, Ugurbil K, Kim S-G. Functional magnetic resonance imaging of the retina. *Invest. Ophthalmol. Vis. Sci.* 2002; 43: 1176–1181.
19. Sicard K, Shen Q, Brevard ME, Sullivan R, Ferris CF, King JA, Duong TQ. Regional cerebral blood flow and BOLD responses in conscious and anesthetized rats under basal and hypercapnic conditions: implications for functional MRI studies. *J. Cereb. Blood Flow Metab.* 2003; 23: 472–481.
20. Duong TQ, Muir ER. Magnetic resonance imaging of the retina. *Jpn. J. Ophthalmol.* 2009; 53: 352–367.
21. Schaeffel F, Burkhardt E. Pupillographic evaluation of the time course of atropine effects in the mouse eye. *Optom. Vis. Sci.* 2005; 82: 215–220.
22. Trinavarat A, Pitusung A. Effective pupil dilatation with a mixture of 0.75% tropicamide and 2.5% phenylephrine: a randomized controlled trial. *Indian J. Ophthalmol.* 2009; 57: 351–354.
23. Liu ZM, Schmidt KF, Sicard KM, Duong TQ. Imaging oxygen consumption in forepaw somatosensory stimulation in rats under isoflurane anesthesia. *Magn. Reson. Med.* 2004; 52: 277–285.
24. Sicard KM, Duong TQ. Effects of hypoxia, hyperoxia and hypercapnia on baseline and stimulus-evoked BOLD, CBF and CMRO₂ in spontaneously breathing animals. *Neuroimage.* 2005; 25: 850–858.
25. Masamota K, Kim T, Fukuda M, Wang P, Kim S-G. Relationship between neural, vascular, and BOLD signals in isoflurane-anesthetized rat somatosensory cortex. *Cerebr. Cortex.* 2007; 17: 942–950.
26. Weber R, Ramos-Cabrer P, Wiedermann D, van Camp N, Hoehn M. A fully noninvasive and robust experimental protocol for longitudinal fMRI studies in the rat. *Neuroimage.* 2006; 29: 1303–1310.
27. Zhao F, Zhao T, Zhou L, Wu Q, Hu X. BOLD study of stimulation-induced neural activity and resting-state connectivity in medetomidine-sedated rat. *Neuroimage.* 2008; 39: 248–260.
28. Yacoub E, Shmuel A, Pfeuffer J, Van De Moortele PF, Adriany G, Andersen P, Vaughan JT, Merkle H, Ugurbil K, Hu X. Imaging brain function in humans at 7 Tesla. *Magn. Reson. Med.* 2001; 45: 588–594.
29. Muir ER, Duong TQ. MRI of retinal and choroidal blood flow with laminar resolution.
30. Nair G, Tanaka Y, Nagaoka T, Pardue MT, Olson DE, Thule PM, Duong TQ. Layer-specific blood-volume MRI of the retina. *Proc. Internat. Soc. Magnetic Reson. Med.* 2008; 158.